Somatic *GJA4* mutation in intracranial extra-axial cavernous hemangiomas

Ran Huo,[1,2] Yingxi Yang,[3] Hongyuan Xu,[1,2] Shaozhi Zhao,[1,2] Dong Song,[4] Jiancong Weng,[5] Ruochen Ma,[4] Yingfan Sun,[1,2] Jie Wang,[1,2] Yuming Jiao [ID] ,[1,2] Junze Zhang,[1,2] Qiheng He [ID] ,[1,2] Ruolei Wu,[6] Shuo Wang,[1,2] Ji-Zong Zhao,[1,2] Junting Zhang,[1,2] Jiguang Wang,[3,4,7] Yong Cao [ID] [1,2,8]

ABSTRACT

Objective Extra-axial cavernous hemangiomas (ECHs) are sporadic and rare intracranial occupational lesions that usually occur within the cavernous sinus. The aetiology of ECHs remains unknown.

Methods Whole-exome sequencing was performed on ECH lesions from 12 patients (discovery cohort) and droplet digital polymerase-chain-reaction (ddPCR) was used to confirm the identified mutation in 46 additional cases (validation cohort). Laser capture microdissection (LCM) was carried out to capture and characterise subgroups of tissue cells. Mechanistic and functional investigations were carried out in human umbilical vein endothelial cells and a newly established mouse model.

Results We detected somatic *GJA4* mutation (c.121G>T, p.G41C) in 5/12 patients with ECH in the discovery cohort and confirmed the finding in the validation cohort (16/46). LCM followed by ddPCR revealed that the mutation was enriched in lesional endothelium. In vitro experiments in endothelial cells demonstrated that the *GJA4* mutation activated SGK-1 signalling that in turn upregulated key genes involved in cell hyperproliferation and the loss of arterial specification. Compared with wild-type littermates, mice overexpressing the *GJA4* mutation developed ECH-like pathological morphological characteristics (dilated venous lumen and elevated vascular density) in the retinal superficial vascular plexus at the postnatal 3 weeks, which were reversed by an SGK1 inhibitor, EMD638683.

Conclusions We identified a somatic *GJA4* mutation that presents in over one-third of ECH lesions and proposed that ECHs are vascular malformations due to *GJA4*-induced activation of the SGK1 signalling pathway in brain endothelial cells.

WHAT IS ALREADY KNOWN ON THIS TOPIC

⇒ Extra-axial cavernous hemangiomas (ECHs) are rare intracranial lesions. The genetic cause of this disorder is unknown. The somatic *GJA4* mutation was ever reported in hepatic hemangiomas, dural angioleiomyomas, orbital cavernous venous malformations and so on.

WHAT THIS STUDY ADDS

⇒ We identified a somatic *GJA4* mutation in ECHs, which promoted ECs hyperproliferation and inhibited arterial specification through SGK1 pathway.

HOW THIS STUDY MIGHT AFFECT RESEARCH, PRACTICE OR POLICY

⇒ We represented an SGK1 inhibitor as a candidate for pharmacotherapeutics of this rare disease.

INTRODUCTION

Extra-axial cavernous hemangiomas (ECHs) are rare intracranial lesions,[1] mostly in the cavernous sinus (represent 3% of all benign cavernous sinus lesions)[2] and occasionally in dural sinuses.[3–5] ECHs are primarily detected as solitary lesions in individuals without family history. These lesions grow over time, distorting and compressing adjacent tissues—a behaviour similar to neoplastic lesions. The aetiology of ECHs remains elusive, and it is controversial whether these lesions should be considered as vascular tumours or vascular malformations. Histologically, ECHs have similarities with cerebral cavernous malformations (CCMs),[6] both presenting with a network of thin-walled dilated vessels, lined by a single layer of endothelial cells. The vessels are often adjacent to each other, but fibrous connective tissue may separate them. CCMs are vascular malformations in the central nervous systems caused by germline mutations in CCM complex (familial CCMs)[7] and/or somatic mutations in *PIK3CA*, *MAP3K3* or other genes (sporadic CCMs).[8] The histological similarities between ECHs and CCMs indicate that a genetic cause may underlie the development of ECHs. So we sought to identify somatic mutations in the cranial vasculature that contribute to ECH lesions and present candidates for pharmacotherapeutics of the rare disease.

METHODS AND MATERIALS
Patients

This study enrolled patients diagnosed as intracranial ECHs according to standard procedure, confirmed by a panel of radiologists, neurosurgeons and pathologists. These patients had neither exposure to cranial radiation nor documented family history of

relevant disorders such as cavernous hemangiomas or genetic vascular diseases.

Genomic analysis

The discovery cohort included patients with fresh surgical lesions and paired peripheral blood, as well as patients with formalin-fixed paraffin-embedded (FFPE) specimens. Whole-exome sequencing (WES) with paired-end 150 bp reads was carried out in ECH lesions (300×) and blood controls (100×) to detect somatic mutations in the discovery cohort. An updated SAVI2[9] pipeline was leveraged for variant discovery and prioritisation. The validation cohort comprised FFPE samples from additional patients with ECH. QX200 ddPCR was performed to orthogonally verify *GJA4* mutations.

Clinical relevance and protein structural analysis

The MRI and pathological images of patients were obtained from the Beijing Tiantan Hospital imaging system. According to MRI characteristics, ECH lesions were divided into sponge-like type (bright homogeneous enhancement) and mulberry-like type (heterogeneous enhancement).[10] For the pathological classifications, ECH lesions were divided into two types.[11] Type A lesions have a large number of thin-walled vascular sinusoids, with a single layer of endothelium-lined capillaries and few connective tissues. Type B lesions have numerous irregular vascular spaces, a well-formed vasculature, and connective tissues. Clinicopathological variables and radiographic appearance were used to train a decision tree model for predicting mutation status of *GJA4*. The identified protein conservation analysis and structural modelling were performed. For more specific information, see online supplemental appendix 1.

Cellular and molecular studies

We manipulated gene expression of human umbilical vein endothelial cells (HUVECs) using lentivirus to investigate the function of mutant *GJA4 in vitro*.[12] Western blotting was used for the molecular studies to investigate the function of mutant *GJA4*. Details about the tissue samples and cellular studies were provided in online supplemental appendix 1.

Animals and adeno-associated virus injection

All experiments performed with animals were approved by the Animal Welfare Ethics Committee of Beijing Neurosurgical Institute. One-day-old C57BL/6 mice received a single retro-orbital intravenous injection of 3×10^{10} AAV-control, AAV-*GJA4*-wild-type or AAV-*GJA4*-mutant as described previously.[13] For EMD638683 experiments, 2-week-old C57BL/6 mice that were injected with AAV-*GJA4* G41C at P1 received oral gavage with 600 mg/kg body weight EMD638683 for a week. More details and the methods of retinal staining are provided in online supplemental appendix 1.

Statistical analysis

Two-sided Fisher's exact test was performed to measure the relationships between clinical features and *GJA4* mutation status. The comparisons among more than two groups were performed by one-way analysis of variance followed by Tukey's multiple comparisons test.

RESULTS

Patients

From January 2021 to August 2021, 12 patients with ECH were enrolled in the discovery cohort. Of the 12 patients, 4 had surgical fresh-frozen specimens accompanied by paired peripheral whole blood samples, while 8 had FFPE samples. Forty-six additional patients with ECH from July 2017 to January 2021 with FFPE samples were recruited in the validation cohort. Detailed information of patients is shown in online supplemental table S1.

Detection of somatic *GJA4* c.121G>T mutation

To characterise the genetic variants of ECHs, WES was performed on 12 surgically resected patients in the discovery cohort (figure 1). Using SAVI2[9] on the four fresh-frozen cases (N55-N58) in comparison to the matched blood control, we identified 34 somatic mutations in 30 genes (online supplemental table S2). Notably, only *GJA4* mutation (c.121G>T, p.G41C) was recurrent in two patients (N57 and N58) (figure 1). Moreover, we found the same *GJA4* c.121G>T mutation in other three (N20, N29 and N31) out of eight FFPE samples. Taken together, we identified *GJA4* c.121G>T in 5/12 ECH lesions (41.7%) with the mutational allele frequency ranging from 6% to 14%. Interestingly, prior studies also reported the occurrence of this mutation in hepatic hemangiomas, cutaneous venous malformations, soft tissue angioleiomyomas, dural angioleiomyomas and orbital cavernous venous malformations.[14–16]

Validation of recurrent somatic *GJA4* c.121G>T

To verify the presence of somatic *GJA4* c.121G>T mutation, we first used ddPCR on samples in the discovery cohort. All five *GJA4* c.121G>T mutant cases (two fresh-frozen and three FFPE samples) detected by WES were confirmed by ddPCR (figure 1 and online supplemental figure S1A). No *GJA4* c.121G>T mutation was detected in the remaining ECH samples or any blood controls. We then applied the same method in an independent validation cohort that included 46 ECHs. We discovered the *GJA4* mutation in 16 out of 46 FFPE samples (34.8%), with fractional abundance spanning from 7.53% to 31.37% (figure 1 and online supplemental figure S1 and online supplemental table S3). No *GJA4* mutations were detected in the control series of normal superficial temporal artery obtained from seven individuals who underwent standard craniotomy procedures. Overall, we identified somatic *GJA4* c.121G>T mutation in 21 of 58 ECHs (36.2%).

Clinical relevance of *GJA4* C.121G>T

To reveal clinical relevance of the mutation, we combined discovery and validation cohorts to conduct the correlation analyses (N=58). According to the pathological classifications in a previous study regarding cavernous
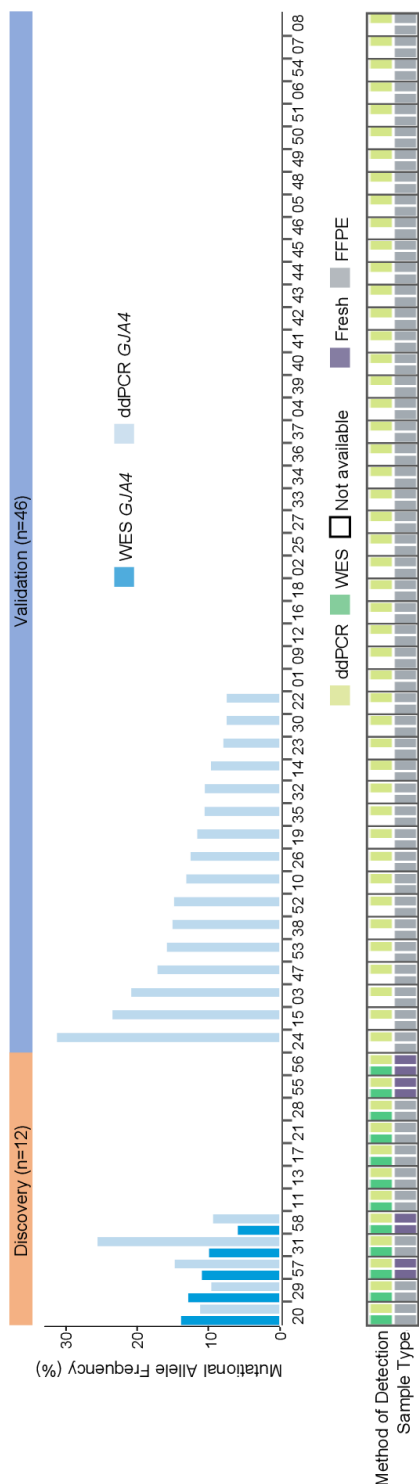
Figure 1 Detection of somatic *GJA4* c.121G>T in human ECHs. The top waterfall plot shows the allele frequencies of *GJA4* c.121G>T mutation, identified by either the percentage of sequence reads that contained variants on WES or the fractional abundance of variants on ddPCR analysis, in human ECHs. The bottom chart shows details about the samples, including the detected technique, the presence or absence of a paired blood sample, and sample type (fresh-frozen or formalin-fixed, paraffin-embedded tissue). ddPCR, digital droplet PCR; ECH, extra-axial cavernous hemangioma; FFPE, formalin-fixed paraffin-embedded; WES, whole-exome sequencing.

sinus hemangiomas,[11] we classified all enrolled patients into two subtypes (Type A and Type B) based on pathological characteristics (figure 2A,B and online supplemental figure S2). The newly detected *GJA4* c.121G>T mutation presented in 45.5% (20/44) of Type B cases, while only 7.1% (1/14) of the Type A ECHs (OR: 10.8, p=0.01). Based on the MRI characteristics of contrast-enhanced T1-weighted sequence (T1WI+C, n=57, patient N28 lacked contrast-enhanced T1-weighted imaging), ECHs were classified as sponge-like lesions or mulberry-like lesions (figures 2C and 3) as previously described.[10] Remarkably, this mutation was considerably enriched in mulberry-like lesions (16/17, 94.1%); and in sharp contrast, we found the mutation in only 5 out 40 (12.5%) sponge-like lesions (OR: 112.0, p=5.29×10⁻⁹), demonstrating a close connection between somatic genotype and imaging appearance of ECH lesions. Moreover, the *GJA4* mutation showed higher prevalence in male compared with female patients (OR: 3.7, p=0.03, figure 2D), and less prevalence on cavernous sinus than other locations (OR: 0.20, p=0.02). Integrating the non-invasive clinical features (pathological subtyping was excluded as it relies on surgical samples), we developed a decision tree model for inferring *GJA4* genotype (figure 2E), which yielded an area under the curve (AUC) of 0.91 (95% CI 0.83 to 0.98) based on fivefold cross validation (online supplemental figure S1B). The results suggest that our model can predict the *GJA4* genotype based on patient gender and radiographic properties of patients with ECH by a non-invasive way.

Structure-based analyses of the *GJA4* mutation

To explore the influence of *GJA4* (Cx37) p.G41C on protein function, we did multiple alignment for Cx37 sequences from human and 44 other vertebrates and found that the mutated position is highly conserved among mammals and birds, and only a few fishes show small hydrophobic residue such as Ala or Val on the position (online supplemental figure S4A). From alpha-fold2[17] predicted 3D structure of the p.G41C Cx37 monomer, we observed the p.G41C mutation is located on the boundary of extracellular loop 1 (ECL1 domain) and transmembrane 1 (TM1 domain) presenting short distance to Ile75 and Trp45 residue (online supplemental figure S4B). Subsequently, we docked 12 Cx37 monomers together and constructed the structural model of a Cx37 gap junction channel between two cells (online supplemental figure S4C). Particularly, the predicted Cx37 gap junction channel structure showed the p.G41C variant is close to the inner side of the channel, which might affect the permeability or selectivity of the Cx37 channel.

Enrichment of *GJA4* c.121G>T in ECH endothelium

We next sought to investigate whether the identified mutation resides in a specific cell type of ECHs. For this purpose, we used LCM technique to separate endothelial cells from non-endothelial cells in FFPE lesions from three patients with ECH (N23, N32, N57; all have
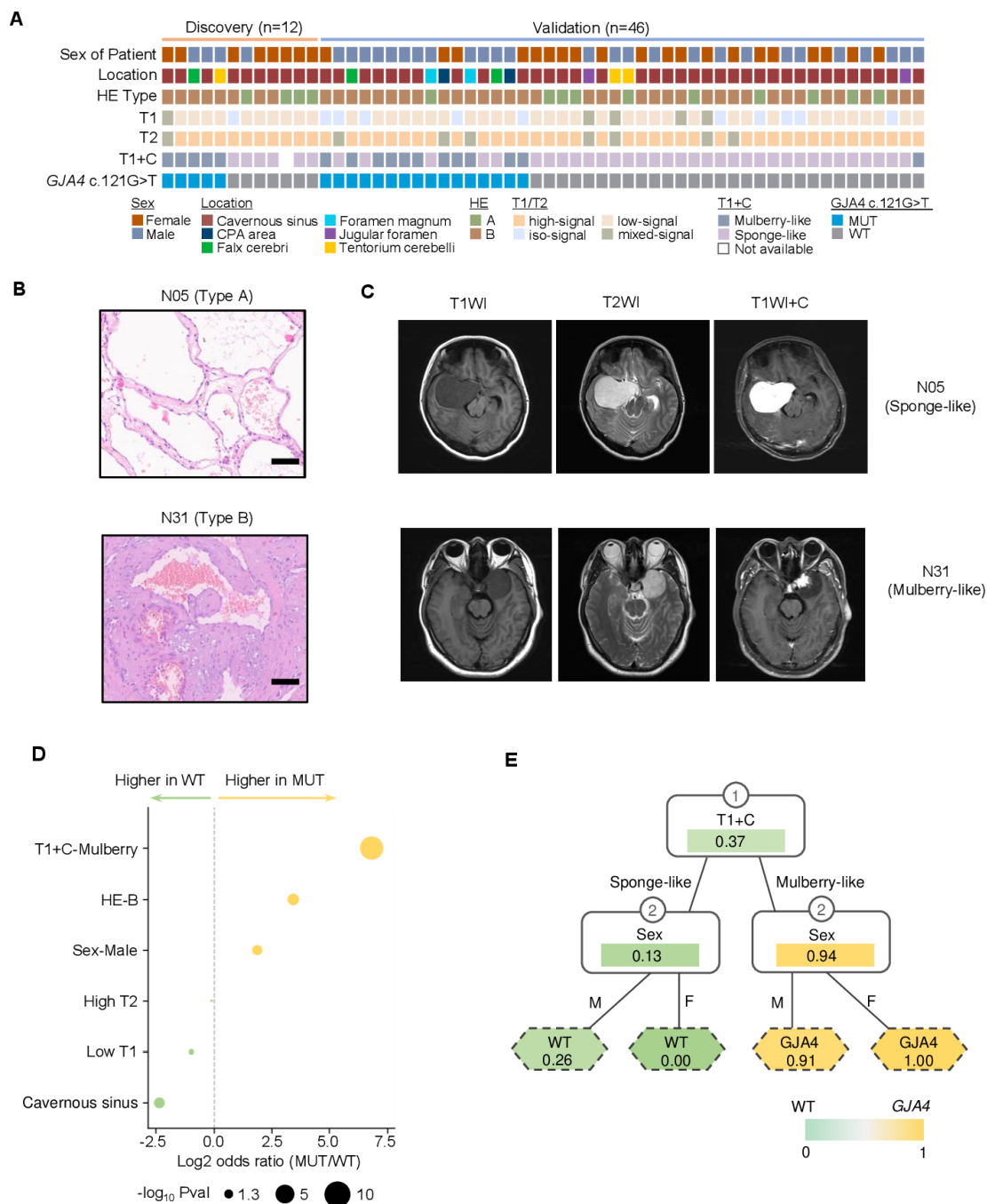
Figure 2 Clinical relevance of somatic *GJA4* mutational status. (A) Clinical characteristics of ECHs, including the sex of the patient, ECH location, HE subtypes, MRI-T1WI, T2WI, T1WI+C and the specific *GJA4* mutation detected. The patient order is consistent with figure 1. (B) Pathological characteristics of ECH lesions. Scale bar: 100 μm. (C) The MRI characteristics of ECHs. (D) The correlation between clinical features and *GJA4* c.121G>T mutation. P value was calculated by Fisher's exact test. Panel E shows the two-step decision tree model to predict *GJA4* c.121G>T mutation. Probability of the mutation was labelled in each node. ECH, extra-axial cavernous hemangioma.

GJA4 c.121G>T). Next, we used ddPCR to quantify the mutation frequency of the two captured cellular components (online supplemental figure S5A). The result of ddPCR analysis revealed that the endothelial cells exhibited significantly increased mutational abundance (10.07%–22.12%), compared with non-endothelial cells (0.00%–3.44%), directly supporting the notion that *GJA4*

mutation resides in lesional endothelium (online supplemental figure S5B).

SGK-1 activation in ECHs with *GJA4* c.121G>T mutation
To further investigate downstream pathways regulated by the *GJA4* mutation, we manipulated HUVECs and examined phosphorylation and protein expression
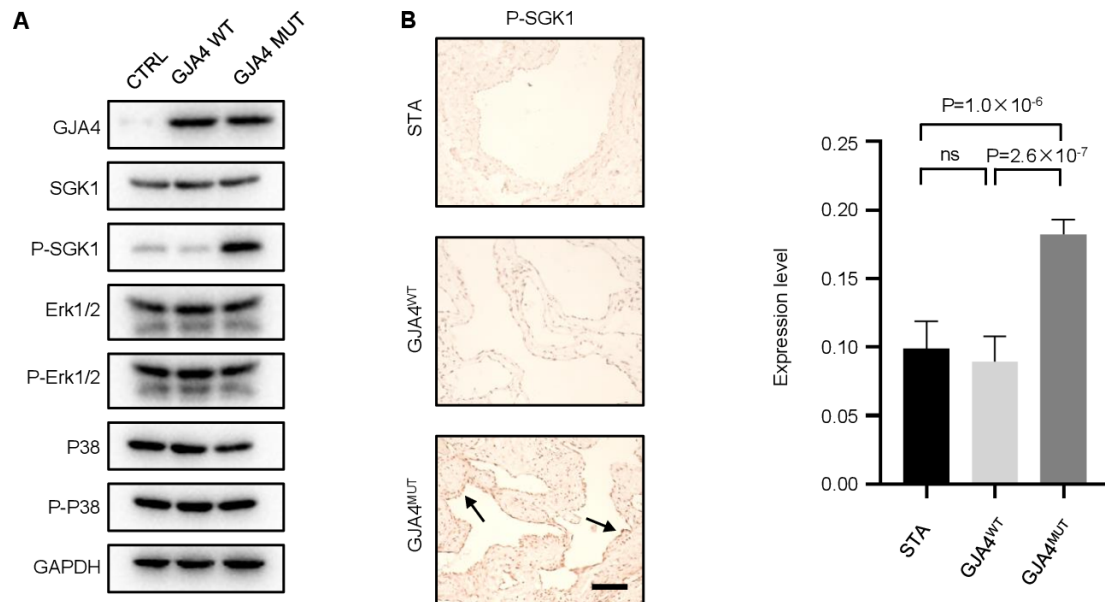
Figure 3 Detection of SGK1 phosphorylation in HUVECS cultures and tissue samples. (A) Immunoblots of HUVECs infected by lentivirus encoding *GJA4*-WT or *GJA4* c.121G>T mutation or empty vector (CTRL) and showed increased phosphorylation of SGK1 but not ERK1/2 or p38. (B) Immunohistochemical staining of a tissue sample of ECH with a *GJA4* mutation shows strong staining for SGK1 phosphorylation in endothelial cells lining the vascular lumen (arrows), whereas non-*GJA4* mutant sample and superficial temporal artery show little or no staining for SGK1 phosphorylation in endothelial cells (arrowheads). Scale bar: 200 μm. The histogram shows semiquantitative grading of p-SGK1 expression levels in *GJA4*-WT, *GJA4* c.121G>T mutation ECHs and STA. One-way ANOVA followed by Tukey's multiple comparisons test was used. ANOVA, analysis of variance; ECH, extra-axial cavernous hemangioma; HUVECs, human umbilical vein endothelial cells; STA, superficial temporal artery.

changes of MAPK signalling, which is regarded as closely related to vascular malformations.[8 18] Specifically, lentivirus was used to infect HUVECs for overexpressing mutant (c.121G>T) and wild-type *GJA4*. We found that compared with endothelial cells infected by lentivirus with an empty vector, no significant difference was observed in MAPK pathways including ERK1/2 and p38 phosphorylation in HUVECs overexpressing mutant or wild-type *GJA4* (figure 3A). A previous study indicated that *GJA4* c.121G>T mutation is able to activate serum and glucocorticoid-induced protein kinase 1 (SGK1) signalling pathway in the HUVECs.[14] SGK-1 is a member of the 'AGC' subfamily of protein kinases, which shares structural and functional similarities with the AKT family of kinases and displays serine/threonine kinase activity. Aberrant expression of SGK1 has profound cellular consequences and is closely correlated with human cancer.[19] We therefore investigated SGK-1 in lentivirus-infected HUVECs and found significantly increased SGK-1 phosphorylation in endothelial cells expressing mutant *GJA4*, compared with those with empty vector or wild type *GJA4* (figure 3A). In order to further investigate the activation of SGK1 in the ECHs, immunohistochemical staining was performed in the ECH surgical samples with and without *GJA4* c.121G>T mutation. Normal superficial temporal artery samples were used as control. The expression for SGK-1 phosphorylation in endothelial cells of the *GJA4*-mutant samples was significantly higher than that of either *GJA4*-WT or normal controls (figure 3B). The results

suggested that *GJA4* c.121G>T mutation was able to activate the SGK-1 signalling in the endothelial cells in the ECHs.

Phenotype of endothelial cells infected by lentivirus with *GJA4* c.121G>T

Recent studies suggest that *GJA4* plays a key role in angiogenesis by modulating endothelial cell proliferation and differentiation.[20–22] It was proposed that fluid shear stress at arterial flow magnitudes maximally activates NOTCH signalling, which in turn upregulates *GJA4* (Cx37) and eventually leads to suppression of endothelial cell proliferation and promotion of arterial specification.[22] To explore the phenotype of endothelial cells with mutant *GJA4* c.121G>T, we infected HUVECs with mutant *GJA4* c.121G>T, wild type *GJA4* or an empty expression lentivirus. The western blot showed that *GJA4* c.121G>T mutant significantly promoted the expression of the common proliferation markers (TK, PCNA and Cyclin D1) in the HUVECs overexpressed with *GJA4* mutation while inhibition of the SGK1 pathway by a SGK1 inhibitor, EMD638683,[23] reversed the process (figure 4A, online supplemental figures S6A,B). Notably, the *GJA4* mutation downregulated the arterial specification markers, including Ephrin-B2 and VEGFR2 in manipulated HUVECs, which were also reversed by EMD638683 via inhibition of SGK1 (figure 4B, online supplemental figure S6C,D). To further validate the above observations in the surgical samples, immunohistochemical staining
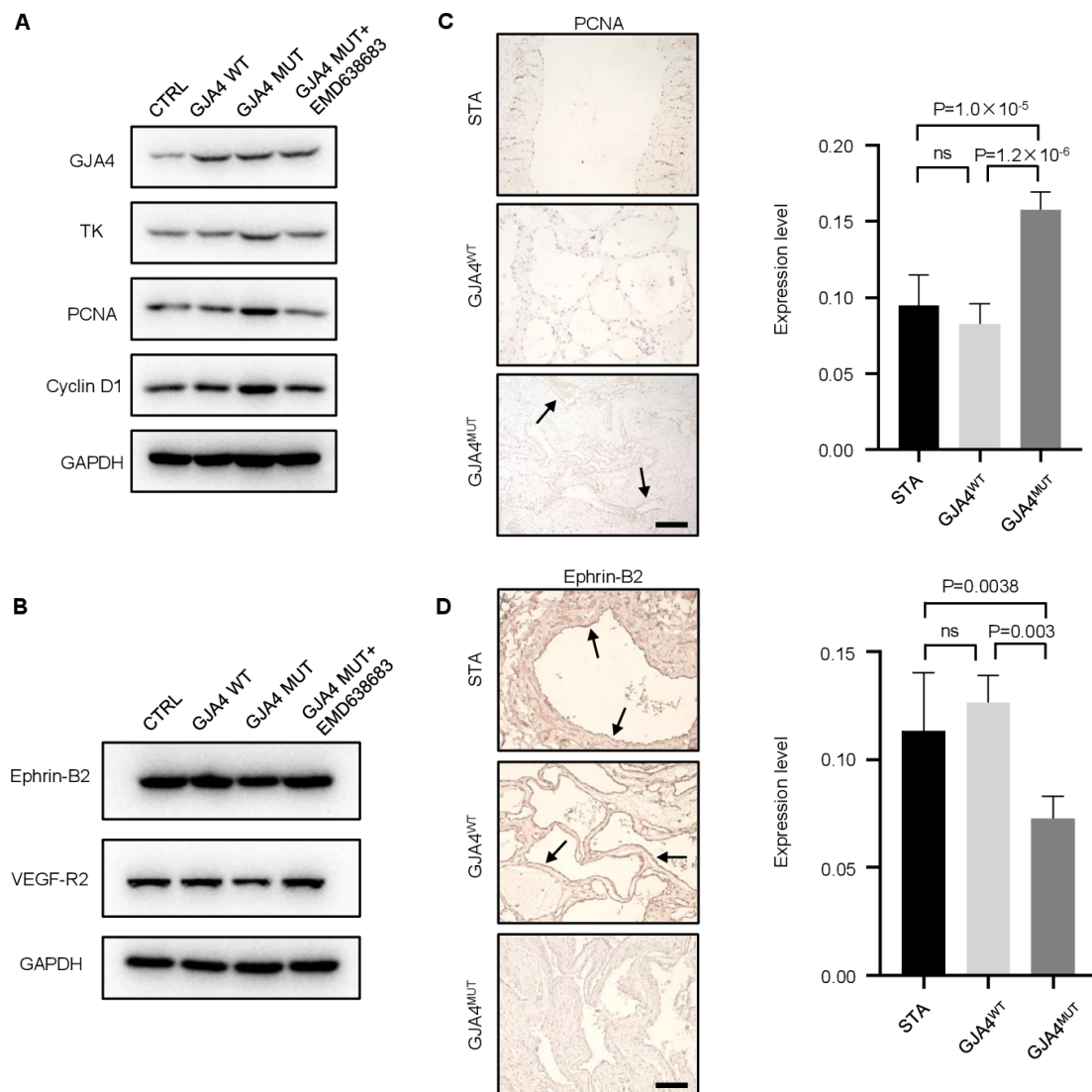
Figure 4 Phenotype of endothelial cells infected with *GJA4* c.121G>T mutant lentivirus. (A) Western blot of TK, PCNA and Cyclin D1 in HUVECs infected with CTRL lentivirus, HUVECs overexpressing wild type *GJA4*, HUVECs overexpressing *GJA4* G41C, HUVECs overexpressing *GJA4* G41C treated with EMD638683. Results from one representative experiment out of three are shown. (B) Western blot of Ephrin-B2 and VEGF-R2 in HUVECs infected with CTRL lentivirus, HUVECs overexpressing wild type *GJA4*, HUVECs overexpressing *GJA4* G41C, HUVECs overexpressing *GJA4* G41C treated with EMD638683. Results from one representative experiment out of three are shown. (C) Immunohistochemical staining of a tissue sample of ECH with a *GJA4* mutation shows increased level of PCNA in endothelial cells lining the vascular lumen (arrows), whereas non-*GJA4* mutant sample and superficial temporal artery show little or no staining for PCNA in endothelial cells. Scale bar: 200 µm. (D) Immunohistochemical staining of a tissue sample of ECH with a *GJA4* mutation shows decreased level of Ephrin-B2 in endothelial cells lining the vascular lumen, whereas non-*GJA4* mutant sample and superficial temporal artery show strong staining for Ephrin-B2 in endothelial cells (arrows). Scale bar: 200 µm. One-way ANOVA followed by Tukey's multiple comparisons test was used. ANOVA, analysis of variance; ECH, extra-axial cavernous hemangioma; HUVECs, human umbilical vein endothelial cells; PCNA, proliferating cell nuclear antigen.

was performed in ECH lesions with and without *GJA4* mutation, together with normal superficial temporal artery controls. We found that PCNA expression in endothelial cells was significantly higher from the *GJA4*-mutant samples than that of either *GJA4*-WT or control (figure 4C). By contrast, Ephrin-B2 were considerably lower in *GJA4*-mutant samples than that of *GJA4*-WT or control (figure 4D). These results collectively demonstrated that *GJA4* c.121G>T mutation induced endothelial cell hyperproliferation and loss of arterial specification through SGK-1 signalling.

Altered retinal angiogenesis in mice by *GJA4* c.121G>T

ECHs are pathologically characterised by dilated vascular lumens within the venous sinus and abnormal angiogenesis.[3] These lesions, in which dilated veins are filled with blood undergo lifelong slow expansion in the venous sinus, rarely accompanied by bleeding.[24] Therefore,

we investigated the role of the *GJA4* mutation in terms of the pathological morphological characteristics and angiogenesis by using a well-studied model of neonatal murine retinal vascularisation in the postnatal mice leveraging AAV-mediated endothelial-specific overexpression. Specifically, *GJA4*-WT and *GJA4*-mutant were overexpressed in the mouse endothelial cells by AAV injection via retro-orbital sinus at the first day postnatal (P1).

To check whether AAV specifically infected endothelial cells, we used immunofluorescence staining to examine the GFP signal in CD31-positive endothelial cells in the brain, retina and liver. We found that GFP was localised satisfactorily in the CD31 positive cells at the third week postinjection (online supplemental figure S7A), suggesting that AAV successfully induces the target gene expression specifically in the endothelial cells.

We next investigated the expression of SGK1 in the endothelial cells with *GJA4*-mutant in vivo. Since SGK1 is highly expressed in several retinal neuronal cells,[25] the expression of SGK1 in retinal neurons will interfere with the SGK1 signal in the retinal vessels. We conversely investigated the phosphorylation of SGK1 in the brain endothelial cells in the mice receiving retro-orbital intravenous injection of AAV-control, AAV-*GJA4*-wild-type or AAV-*GJA4*-mutant at the post-natal 3 weeks. The results showed that endothelial SGK-1 phosphorylation in *GJA4* mutant mice was significantly increased while in the *GJA4*-WT and control SGK-1 phosphorylation seldom presented (online supplemental figure S7B and S7C).

Finally, we illuminated the morphological changes of retinal vessels in the *GJA4* mutation mice model. The mechanisms of vessel enlargement have been previously identified as local proliferation of endothelial cells, loss of mural cell coverage in the central nervous system (CNS) vasculature, dysfunction of the endothelial cell migration and so on.[26] We found that the retinal vein lumen diameter of *GJA4* c.121G>T overexpression mice was remarkably increased compared with that of control or *GJA4*-WT overexpression mice (figure 5A), while no difference was observed in arterial lumen diameter between mutant group and control or wild-type group (online supplemental figure S7D). The diameter enlargement of retinal vein vessel in *GJA4*-mutant mice was reversed by an administration of a SGK1 inhibitor, EMD638683 (figure 5A). Meanwhile, we assessed retinal vascular network density at the angiogenic front and found increased vascular formation in the mutant group (figure 5B), which was also reversed by the SGK1 inhibitor. To determine whether *GJA4* c.121G>T mutation affects the coverage of mural cells, we performed immunofluorescence staining of mouse retina. The expression of α-SMA (smooth muscle actin), a marker of smooth muscle cells, in the retinal vasculature was significantly decreased in the mutant group, while in the wild-type retinal vasculature, α-SMA was upregulated compared with the control at P21 (figure 5C). When *GJA4*-mutant mice were treated with the SGK1 inhibitor, the retinal vasculature α-SMA was returned to the similar level as control and wild type

(figure 5C). Our results suggested that *GJA4* c.121G>T was able to increase the vein's lumen diameter in the vascular angiogenesis in mice through SGK1 signalling. These morphological changes are consistent with the most prominent pathological features of ECH lesions.

DISCUSSION

In this study, we identified a somatic *GJA4* mutation that was present in more than one-third of tissue samples of ECHs and found that the lesions with the mutation mostly present with mulberry-like lesions on the contrast-enhanced MRI. In vitro functional studies revealed that the *GJA4* mutation was accompanied by dysregulation of the Cx37-SGK1 pathway in the endothelium inducing endothelial cell hyperproliferation and loss of arterial specification. Further in vivo models illuminated abnormal venous angiogenesis, particularly presented by dilated venous lumen in the mutant group. These findings are in line with the fact that other types of vascular malformation are caused by somatic mutations in oncogenic pathways activation in the endothelium.

Recently, various somatic mutations in sporadic vascular diseases have been reported, particularly in vascular malformations including verrucous venous malformations (*MAP3K3* c.1323C>G),[27] extracranial arteriovenous malformations (*MAP2K1*),[28] cerebral arteriovenous malformations (*KRAS* c.35G>T),[18] cerebral cavernous hemangiomas (*MAP3K3* c.1323C>G)[8] and so on. Interestingly, these somatic mutations share similar characteristics, including: (1) specificity in endothelial cells; (2) relatively low mutational allelic frequency; (3) presence as single hotspot mutations activating oncogenic pathways, which can be reversed by targeted drugs (in part restore the normal function and morphology of endothelial cells). In our study, the somatic *GJA4* mutation is consistent with these features implying the vascular malformation nature of ECHs. However, we cannot exclude the possibility of complex single nucleotide polymorphism (SNP) combination or de novo germline variants contributing to ECH pathogenesis. Further genetic research, such as genome wide association study, could be of interest for further ECH investigation.

Previous studies had identified the same somatic *GJA4* mutation (c.121G>T, p.G41C) in other vascular pathologies such as orbital cavernous venous malformations, cutaneous and hepatic vascular lesions and dural angioleiomyoma.[14–16 29] Our study identified this mutation in ECHs and more importantly, we performed correlation analysis between clinical traits and the *GJA4* mutation in a large cohort and revealed that ECH lesions with the *GJA4* mutation mostly present with mulberry-like lesions on the contrast-enhanced MRI and mainly show Type B on pathology. In addition, our study presented in vivo experiments that demonstrated the functional effect of the mutation.

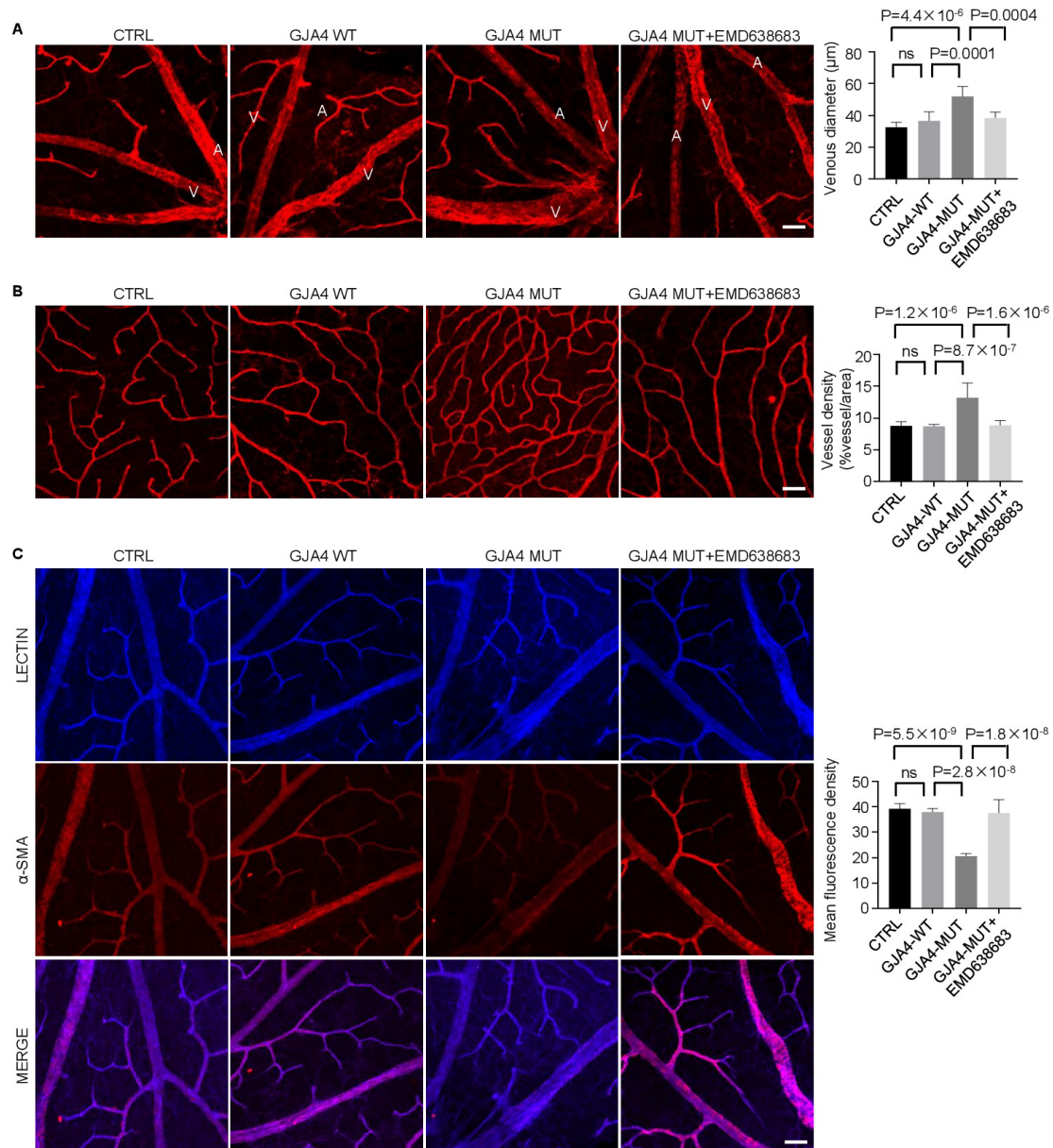In our previous study, we found that *MAP3K3*-I441M mutation in sporadic CCMs most often presents with

Figure 5 *GJA4* mutation regulates retinal angiogenesis in mice. (A) Staining of retinas showed an increase in venous diameter of vessels in the superficial plexuses in the retina of *GJA4*-mutant mice, compared with *GJA4*-WT and CTRL mice. EMD638683 reversed the increase of venous diameter caused by *GJA4* mutation (n=6). Symbols: A=artery; V=vein. Scale bar: 100 μm. (B) Analysis of Lectin staining (red) at the angiogenic front of C57 mice injected with *GJA4*-WT, *GJA4*-MUT and CTRL AAV revealed *GJA4* mutation increased the vascular density of vessels, which was reversed by EMD638683 (n=8). Scale bar: 100 μm. (C) Immunostaining showed a reduced α-SMA (red) expression in the vascular networks of retinas of *GJA4*-mutant mice compared with that observed in *GJA4*-WT and CTRL mice. Meanwhile, the expression of α-SMA was increased in *GJA4*-mutant mice treated with EMD638683 (n=3). Scale bar: 100 μm. One-way ANOVA followed by Tukey's multiple comparisons test was used. ANOVA, analysis of variance.

popcorn-like lesions on the MRI as the Zabramski classification type II.[8] Several research demonstrated that somatic GOF mutations in *PIK3CA* are present in both sporadic and familial CCMs, whose lesions have manifested more aggressive (progressive growth or haemorrhage) on the MRI.[30 31] In our current study, we demonstrated a close relationship between mulberry-like MRI classification and the *GJA4* mutations. All these investigations imply that somatic mutations in the vascular malformations may be more likely to form specific imaging patterns and

the imaging-based diagnosis could be possible to infer genetic mutations in the vascular malformations. An interpretable decision tree model for evaluating molecular aetiology via MRI and clinical features for patients with ECH provides a non-invasive way of precision disease diagnosis.

In our model, we observed abnormal vascular phenotypes in the retina, but no obvious abnormalities have been detected in the brain. This might be because, in contrast to brain vessels, the mouse retinal vasculature

does not fully mature until 3 weeks after birth while the abnormal angiogenesis is more likely to be induced in the immature vasculature.[32] We acknowledge this limitation and further studies are needed to induce the *GJA4* mutation at an earlier stage in mice for potential detection of brain vascular morphology. In addition, Hongo study found that as a gain-of-function mutation, *GJA4* G41C leads to formation of a hyperactive hemichannel and overexpression of the mutant protein in HUVECs resulted in a loss of cellular integrity and impaired tube formation.[16] Yet, Simon *et al* generated Cx37-/-Cx40-/- animals and showed that these animal displayed dilated vessel and subcutaneous bleeding.[33] These studies collectively demonstrated the importance of accurate dose of *GJA4* gene for vascular function. Moreover, we believe that the *GJA4* c.121G>T mutation is not simply enhancing *GJA4* function. Instead, the mutation should lead to *GJA4* function changes.

Current treatment for ECHs is neurosurgical excision or radiotherapy of the symptomatic lesions. However, surgical intervention is associated with high cost and significant risks, particularly when the lesion involves critical brain regions. Meanwhile, the efficacy of radiotherapy is variable and unsatisfactory: the volume reduction rate of ECHs after radiotherapy ranges from 0% to 86%.[34 35] Therefore, the pharmacotherapeutics are urgently needed in this disease. In our study, we found that the *GJA4* mutation upregulated the Cx37-SGK1 pathway in the endothelium, leading to abnormal proliferation of endothelium and the inhibition of artery specification. We demonstrated that administration of a pharmacological inhibitor of SGK1 was able to reverse these phenotypes and partially restored vascular morphology. Results from mouse model suggested that ECH is a potentially medically treatable disorder. In light of multiple roles of SGK1 in carcinogenesis, tumour progression and radioresistance,[19 36] several specific and selective inhibitors of SGK1 have been recently developed. In the absence of direct pharmacological inhibitors of the *GJA4* mutation, small-molecule SGK1 inhibitors with antitumour and reducing radioresistance effects represent candidates for clinical trials in the treatment of ECHs. Besides the SGK-1 inhibitor EMD638683, some other inhibitors such as Carbenoxolone (shown to accelerate the rate of healing of both gastric and duodenal ulcer)[37] or Spironolactone (used for hypertension, oedema and primary aldosteronism)[38] have been previously used to counteract the vascular malformations induced by the *GJA4* somatic mutation (c.121G>T, p.G41C).[14 16] However, none of these inhibitors are currently used clinically in the treatment of ECHs. Further study is needed to verify the safety and efficacy of these inhibitors.

Author affiliations
[1]Department of Neurosurgery, Beijing Tiantan Hospital, Capital Medical University, Beijing, China
[2]China National Clinical Research Center for Neurological Diseases, Beijing, China
[3]Department of Chemical and Biological Engineering, The Hong Kong University of Science and Technology, Hong Kong, China
[4]Division of Life Science, Center for Systems Biology and Human Health and State Key Laboratory of Molecular Neuroscience, The Hong Kong University of Science and Technology, Hong Kong, China
[5]Department of Neurosurgery, China-Japan Friendship Hospital, Beijing, China
[6]School of Medical Technology, Beijing Institute of Technology, Beijing, China
[7]Hong Kong Center for Neurodegenerative Diseases, InnoHK, Hong Kong SAR, China
[8]Beijing Neurosurgical Institute, Capital Medical University, Beijing, China

ORCID iDs
Yuming Jiao http://orcid.org/0000-0001-8351-4602
Qiheng He http://orcid.org/0000-0001-6715-298X
Yong Cao http://orcid.org/0000-0002-8289-1120

REFERENCES
1 Biondi A, Clemenceau S, Dormont D, *et al*. Intracranial extra-axial cavernous (hem) angiomas: tumors or vascular malformations? *J Neuroradiol* 2002;29:91–104.
2 Linskey ME, Sekhar LN. Cavernous sinus hemangiomas: a series, a review, and an hypothesis. *Neurosurgery* 1992;30:101–8.
3 Meyer FB, Lombardi D, Scheithauer B, *et al*. Extra-Axial cavernous hemangiomas involving the dural sinuses. *J Neurosurg* 1990;73:187–92.
4 Melone AG, Delfinis CP, Passacantilli E, *et al*. Intracranial extra-axial cavernous angioma of the cerebellar falx. *World Neurosurgery* 2010;74:501–4.
5 Beskonakli E, Kaptanoglu E, Okutan O, *et al*. Extra-Axial cavernomas of the cerebellopontine angle involving the seventh-eighth nerve complex. *Neurosurg Rev* 2002;25:222–4.

6 Naik S, Phadke RV, Taunk A, *et al*. Dynamic contrast-enhanced magnetic resonance imaging in diagnosis of cavernous hemangioma of cavernous sinus. *Journal of Neurosciences in Rural Practice* 2017;08:311–3.

7 Zafar A, Quadri SA, Farooqui M, *et al*. Familial cerebral cavernous malformations. *Stroke* 2019;50:1294–301.

8 Weng J, Yang Y, Song D, *et al*. Somatic map3k3 mutation defines a subclass of cerebral cavernous malformation. *Am J Hum Genet* 2021;108:942–50.

9 Trifonov V, Pasqualucci L, Tiacci E, *et al*. SAVI: a statistical algorithm for variant frequency identification. *BMC Syst Biol* 2013;7 Suppl 2(Suppl 2):S2.

10 Zhou L-F, Mao Y, Chen L. Diagnosis and surgical treatment of cavernous sinus hemangiomas: an experience of 20 cases. *Surg Neurol* 2003;60:31–6;

11 Shi JX, Hang CH, Pan YX, *et al*. Cavernous hemangiomas in the cavernous sinus. *NEUROSURGERY* 1999;45:1308–13;

12 Li H, Nam Y, Huo R, *et al*. De novo germline and somatic variants convergently promote endothelial-to-mesenchymal transition in simplex brain arteriovenous malformation. *Circ Res* 2021;129:825–39.

13 Chai Z, Sun J, Rigsbee KM, *et al*. Application of polyploid adeno-associated virus vectors for transduction enhancement and neutralizing antibody evasion. *Journal of Controlled Release* 2017;262:348–56.

14 Ugwu N, Atzmony L, Ellis KT, *et al*. Cutaneous and hepatic vascular lesions due to a recurrent somatic gja4 mutation reveal a pathway for vascular malformation. *Human Genetics and Genomics Advances* 2021;2:100028.

15 Tauziède-Espariat A, Pierre T, Wassef M, *et al*. The dural angioleiomyoma harbors frequent gja4 mutation and a distinct DNA methylation profile. *Acta Neuropathol Commun* 2022;10:81.

16 Hongo H, Miyawaki S, Teranishi Y, *et al*. Somatic gja4 gain-of-function mutation in orbital cavernous venous malformations. *Angiogenesis* 2023;26:37–52.

17 Jumper J, Evans R, Pritzel A, *et al*. Highly accurate protein structure prediction with alphafold. *Nature* 2021;596:583–9.

18 Nikolaev SI, Fish JE, Radovanovic I. Somatic activating KRAS mutations in arteriovenous malformations of the brain. *N Engl J Med* 2018;378:1561–2.

19 Sang Y, Kong P, Zhang S, *et al*. SGK1 in human cancer: emerging roles and mechanisms. *Front Oncol* 2020;10:608722.

20 Fang JS, Angelov SN, Simon AM, *et al*. Cx37 deletion enhances vascular growth and facilitates ischemic limb recovery. *Am J Physiol Heart Circ Physiol* 2011;301:H1872–81.

21 Hamard L, Santoro T, Allagnat F, *et al*. Targeting connexin37 alters angiogenesis and arteriovenous differentiation in the developing mouse retina. *FASEB J* 2020;34:8234–49.

22 Fang JS, Coon BG, Gillis N, *et al*. Shear-induced notch-cx37-p27 axis arrests endothelial cell cycle to enable arterial specification. *Nat Commun* 2017;8:2149.

23 Towhid ST, Liu G-L, Ackermann TF, *et al*. Inhibition of colonic tumor growth by the selective SGK inhibitor emd638683. *Cell Physiol Biochem* 2013;32:838–48.

24 Gonzalez LF, Lekovic GP, Eschbacher J, *et al*. Are cavernous sinus hemangiomas and cavernous malformations different entities? *Neurosurg Focus* 2006;21:e6.

25 Schniepp R, Kohler K, Ladewig T, *et al*. Retinal colocalization and in vitro interaction of the glutamate transporter eaat3 and the serum- and glucocorticoid-inducible kinase sgk1 [correction]. *Invest Ophthalmol Vis Sci* 2004;45:1442–9.

26 Gifre-Renom L, Jones EAV. Vessel enlargement in development and pathophysiology. *Front Physiol* 2021;12:639645.

27 Couto JA, Vivero MP, Kozakewich HPW, *et al*. A somatic map3k3 mutation is associated with verrucous venous malformation. *Am J Hum Genet* 2015;96:480–6.

28 Couto JA, Huang AY, Konczyk DJ, *et al*. Somatic map2k1 mutations are associated with extracranial arteriovenous malformation. *Am J Hum Genet* 2017;100:546–54.

29 Chen K-H, Huang H-Y, Chen T-C, *et al*. A clinicopathological reappraisal of orbital vascular malformations and distinctive gja4 mutation in cavernous venous malformations. *Hum Pathol* 2022;130:79–87.

30 Ren AA, Snellings DA, Su YS, *et al*. Pik3Ca and CCM mutations fuel cavernomas through a cancer-like mechanism. *Nature* 2021;594:271–6.

31 Hong T, Xiao X, Ren J, *et al*. Somatic map3k3 and PIK3CA mutations in sporadic cerebral and spinal cord cavernous malformations. *Brain* 2021;144:2648–58.

32 Stahl A, Connor KM, Sapieha P, *et al*. The mouse retina as an angiogenesis model. *Invest Ophthalmol Vis Sci* 2010;51:2813–26.

33 Simon AM, McWhorter AR. Vascular abnormalities in mice lacking the endothelial gap junction proteins connexin37 and connexin40. *Dev Biol* 2002;251:206–20.

34 Thompson TP, Lunsford LD, Flickinger JC. Radiosurgery for hemangiomas of the cavernous sinus and orbit: technical case report. *Neurosurgery* 2000;47:778–83.

35 Ivanov P, Chernov M, Hayashi M, *et al*. Low-Dose gamma knife radiosurgery for cavernous sinus hemangioma: report of 3 cases and literature review. *Minim Invasive Neurosurg* 2008;51:140–6.

36 Zhou C, Xiao W, Jiang T, *et al*. Targeting sgk1 enhances the efficacy of radiotherapy in locally advanced rectal cancer. *Biomed Pharmacother* 2020;125:109954.

37 Pinder RM, Brogden RN, Sawyer PR, *et al*. Carbenoxolone: A review of its pharmacological properties and therapeutic efficacy in peptic ulcer disease. *Drugs* 1976;11:245–307.

38 Batterink J, Stabler S, Tejani A, *et al*. Spironolactone for hypertension. the cochrane database of systematic reviews. 2010.